Sustainable ferrocene for enhanced heterogeneous photoelectro-Fenton: a novel application in gas diffusion electrodes

Géssica O. S. Santos[a,], Isaac Sánchez-Montes[a], Paulo Jorge M. Cordeiro-Junior[a], Taynara O. Silva[a], Manuel A. Rodrigo[b], Marcos R. V. Lanza[a,*]*

[a]São Carlos Institute of Chemistry, University of São Paulo, São Carlos, São Paulo 13566-590, Brazil

[b]Chemical Engineering Department, Faculty of Chemical Sciences and Technologies, Universidad de Castilla-La Mancha, Ciudad Real, Spain

*** Corresponding authors:**

gessicasantiag@gmail.com (G.O.S. Santos)

marcoslanza@usp.br (M. R.V Lanza)

Abstract

In the present work, the development of a low-cost ferrocene (Fc)-modified gas diffusion electrode (GDE) and its effective application for the treatment of paracetamol-contaminated water have been demonstrated. The electrochemical characterization using the rotating ring disk electrode (RRDE) technique showed a slight decrease in the amount of H_2O_2 detected, probably due to the catalytic conversion of H_2O_2 to •OH by the Fc, which increased the degradation efficiency. Among the current densities tested, 7.5 mA cm^{-2} was found to be the most efficient for paracetamol degradation, balancing energy consumption and treatment efficacy. The addition of UV-A irradiation further enhanced the degradation performance, especially at higher Fc content (15% Fc-GDE), due to the generation of additional •OH species by the interaction between Fc and UV-A light. However, the 5% Fc-GDE proved to be the most cost-effective and efficient electrode, demonstrating optimal energy utilization and total organic carbon (TOC) removal. The low iron leaching observed with the 5% Fc-GDE (0.06 mg L^{-1}) highlights its suitability for sustainable, large-scale applications in neutral water matrices, ensuring safe and efficient degradation of pharmaceutical contaminants for potential reuse, such as in agricultural irrigation.

Keywords: gas diffusion electrode; ferrocene; heterogeneous electro-Fenton; paracetamol; UV-A radiation.

1. Introduction

Water contamination by pharmaceuticals occurs due to a wide range of factors; among these factors include the low efficiency of conventional processes used for the treatment of effluents generated by the pharmaceutical industry and hospitals, and the improper disposal of unused or expired pharmaceutical compounds that find their way into the sewage systems [1-3]. In recent years, there have been huge concerns regarding the potential adverse effects of pharmaceutical contaminants on aquatic ecosystems and human health. Among the contaminants of particular concern is N-acetyl-p-aminophenol, known commercially as paracetamol (PCT) or acetaminophen, which is one of the most widely employed antipyretics and analgesics worldwide. A number of studies reported in the literature have frequently detected the presence of PCT in surface water and drinking water, as well as in wastewater [4].

Electrochemical advanced oxidation processes (EAOP) have been used as an alternative oxidation technology for the removal of pharmaceuticals in complex matrices due to the ability of these processes to destroy refractory organic pollutants – owing particularly to the large amount of hydroxyl radicals (•OH) generated through these processes [5]. Among the EAOPs, the electro-Fenton (EF) process has been found to be notably outstanding due to its higher degradation rates propelled by the *in situ* production of •OH through the reaction of hydrogen peroxide (H_2O_2) generated via the cathodic reduction of oxygen (O_2) (see Eq. 1) and the iron salt added to the solution (called the Fenton reaction) (Eq. 2). The photo-electro-Fenton (PEF) or solar photo-electro-Fenton (S-PEF) process involves the exposure of the solution to irradiation – using artificial UV sources (in PEF) (mainly at λ = 200-400 nm) or natural solar light (in S-PEF), which helps enhance the efficiency of the process.

$$O_2 + 2H^+ + 2e^- \rightarrow H_2O_2 \quad (1)$$

$$H_2O_2 + Fe^{2+} \rightarrow HO\cdot + HO^- + Fe^{3+} \quad (2)$$

However, the classical homogeneous EF process requires the use of an optimum operating pH level (2.0-3.0) and has some underlying drawbacks which are particularly related to the rampant disposal of iron sludge that causes secondary pollution [6]. To help overcome these problems, researchers have sought to use the heterogeneous EF (HEF) process due to its ability to operate in a wide pH range without the need for neutralization of the treated solution, in addition to minimizing the formation of iron sludge and the possibility provided by this process for the reutilization of the heterogeneous catalysts [7, 8]. Carbon-based cathodes modified with iron oxides can be suitably employed as heterogeneous catalysts [9]; under this technique, the supported catalyst can activate the electrogenerated H_2O_2 almost simultaneously. This strategy has recently received considerable attention among researchers because it allows the efficient promotion of Fenton reaction while preventing the dissolution of iron salts [10]. However, despite the advantages of the HEF technique, finding a suitable iron compound to modify carbon matrices in order to obtain the desired material has clearly not been a simple task.

Ferrocene (Fc) is an organometallic compound consisting of Fe(II) coordinated to two cyclopentadienyl rings, forming a "sandwich" structure. This configuration provides Fc with excellent chemical stability, adhering to the 18-electron rule, and enables its good redox reversibility due to its electron donor−acceptor conjugated structure, making it highly suitable for application as a heterogeneous electrocatalyst. In addition, Fc is synthesized through the reaction of cyclopentadienyl sodium with iron(II) chloride, an efficient and environmentally friendly process that supports its classification as a sustainable compound. Combined with its cost-effectiveness, these characteristics establish Fc as an ideal mediator for degrading pharmaceutical contaminants in water, aligning with the principles of green chemistry and sustainable water treatment practices.

Although some studies have investigated the effects of Fc in heterogeneous Fenton reactions for the degradation of dye solutions, issues such as the requirement for acidic

conditions can limit its applicability, particularly in large-scale environmental processes where neutral pH conditions are more desirable [11, 12]. Other studies have explored the application of Fc functionalized with metal-organic frameworks and carbon nitride for the degradation of bisphenol A, as well as with graphene for the oxidation of ciprofloxacin [13, 14]**.** Despite promising results, challenges related to the stability and recyclability of Fc-based catalysts, along with the need for expensive materials, hinder their application. To the best of our knowledge, Fc has not been used as a heterogeneous catalyst in gas diffusion electrodes (GDE). GDEs consist of a conductive, porous, hydrophobic carbon base (adjusted with poly(tetrafluoroethylene)) and a catalytic layer which is positioned in contact with the electrolyte [15].

Compared to planar electrodes, GDEs have become widely popular among researchers due to the following reasons: they are easy to produce, have the ability to operate at high current densities, allow O_2 solubilization in solution, and they are relatively less costly to produce [35,54,73]. With regard to using GDEs for oxygen reduction reaction (ORR) to H_2O_2, O_2 is constantly supplied through the electrode, where the technique leads to the formation of a triple interface (gas-solid-liquid); this system eliminates the problem related to O_2 solubility - which has been reported for planar electrodes, and thus helps improve H_2O_2 production [16].

To the best of our knowledge, this is the first study that has sought to demonstrate the successful fabrication and characterization of Fc modified GDEs and their application for the degradation of persistent pollutants. It is equally worth pointing out that, to date, no study reported in the literature has employed Fc as heterogeneous catalyst for the degradation of PCT. Thus, taking the above considerations into account – given the suitable characteristics of Fc and the inherent constraints encountered under the HEF process, the present study sought to demonstrate the development of a novel gas diffusion electrode (GDE) based on Printex L6 carbon (PL6C) modified with different amounts of

Fc and evaluate the performance and efficiency of the low-cost and environmentally-friendly Fc/PL6C-GDEs when applied as electrocatalysts under the HEF system for the removal of PCT from water. The effectiveness of the proposed HEF system operated using the modified GDEs will be evaluated in terms of the pollutant removal efficiency, mineralization and energy consumption.

2. Materials and Methods

2.1 Chemicals

For the preparation of the GDEs, the following materials were employed: poly(tetrafluoroethylene) (PTFE) - acquired from Dalflon, commercial carbon cloth (model PX30) - obtained from Zoltek, carbon black Printex® L6 (PL6C) - purchased from Evonik Brazil Ltd. [17, 18], and ferrocene – obtained from Sigma-Aldrich (98%). For H_2O_2 electrogeneration and degradation experiments, the following products were employed: paracetamol (analytical grade) – obtained from Labsynth, potassium sulfate (99%), acetonitrile (ACN; HPLC grade) and formic acid (85%) - acquired from Sigma-Aldrich. For the quenching experiments, the following products were used: benzoquinone (BQ) - acquired from Sigma-Aldrich (>98%), isopropyl alcohol (IPA) (99.5%) and ammonium oxalate (AO) (99.5%) - obtained from Vetec. Ultrapure water (Millipore Milli-Q system, resistivity ≥18.2 MΩcm) was used to prepare all aqueous solutions.

2.2 Rotating Ring-Disk Electrode (RRDE) System

First, 1.0 mg of catalyst, which consisted of PL6C with proportions (*w*/*w*) of Fc ranging from 5% to 15%, was dispersed in 1 ml of isopropanol. After that, 25 µL of the dispersion, previously sonicated for 30 min, was carefully placed on a glassy carbon disk electrode (0.2475 cm^2) by dripping. Electrochemical measurements were performed in a three-electrode cell which consisted of a rotating ring disk electrode (RRDE) (specifically, AFE7R9GCPT model, from Pine Instrument), employed as the working electrode, a Pt

sheet used as the counter electrode, and Ag/AgCl (KCl 3 mol L^{-1}) employed as the reference electrode. The RRDE setup consisted of a platinum ring (with geometric area of 0.1866 cm^2) and a glassy carbon disk (0.2476 cm^2) with a manufacturer-specified collection coefficient of 0.37 (information provided by the manufacturer).

For the RRDE disk, linear sweep voltammetry measurements were performed within the potential range of +0.4 to -1.0 V *vs* Ag/AgCl, while a fixed potential of +1.0 V *vs* Ag/AgCl was applied on the RRDE ring, since H_2O_2 oxidation is controlled by mass-transport at this value, allowing its detection. This technique allows simultaneous monitoring of the ORR at the disk and detection of H_2O_2 as an intermediate or product at the ring [19, 20]. The rotation speed of the RRDE was kept constant at 900 rpm during the measurements. The electrolyte employed in these experiments consisted of 0.1 mol L^{-1} K_2SO_4 solution at pH 2.5, adjusted with H_2SO_4. Prior to each experiment, the electrolyte was thoroughly saturated with N_2 or O_2 and kept under the atmosphere during measurements.

2.3 Preparation of Gas Diffusion Electrode (GDE)

To obtain the unmodified GDE a catalytic mass composed of PL6C (*w*/*w*80%) and PTFE (*w*/*w* 20%) was spread over commercial carbon cloth, as previously described by [21]. Briefly, wet catalytic mass was homogenously dispersed over rectangular carbon cloth (geometric area: 120.0 cm^2) using a brush-like device and the material was heated at 120 °C for 15 min. The same procedure was employed in the preparation of 5% Fc-modified GDE (named 5%Fc-GDE) and 5% Fc-modified GDE (15%Fc GDE). For 5%Fc-GDE the catalytic mass was composed of PL6C (*w*/*w*75%), ferrocene (*w*/*w*5%), and PTFE (*w*/*w* 20%), while for 15% Fc-GDE was used PL6C (*w*/*w*65%), ferrocene (*w*/*w*15%), and PTFE (*w*/*w* 20%). The incorporation of Fc in the PL6C matrix was achieved by physical dispersion, where the desired amounts of ferrocene and PL6C were added to a beaker in an isopropyl alcohol solution and kept under stirring for 1h in order to obtain a

homogeneous dispersion. To obtain the electrodes, the spread catalytic mass were hot pressed for 15 min using 0.5 tons (of weight) at 290 °C. After this step, the electrode is carefully removed from the mold and reshaped into a circular shape with a surface area of 20 cm^2.

2.4 Physical characterization

The surface morphology of the GDE electrodes was visualized employing a field emission scanning electron microscope (FE-SEM; Zeiss GeminiSEM 500) and the elemental chemical composition was determined using energy-dispersive X-ray (EDX) spectroscopy coupled to the SEM equipment. X-ray diffraction (XRD) data was carried out using a Bruker-D8 Advance with Cu Kα radiation over a 2Θ range between 10° and 100°, at a scan rate of 0.02° min^{-1}. Contact angle values for each GDE were obtained using an Attension Theta Flex tensiometer, where 3.0 µL of ultrapure water was dripped onto the GDEs surface. The Raman spectra of GDEs were recorded using a SPELEC RAMAN (Metrohm DropSens, S.L.) with a laser source of 532 nm, controlled by the DROPVIEW SPELEC Software. The XPS analysis was performed on a PHOIBOS 150 AD-CMOS power analyzer (SPECS, model: FleXPS) with a non-monochromatic kα operating at 300 W and 14 kV. The nitrogen adsorption-desorption analysis was performed using a V-Sorb 2800P gas analyzer (Gold APP Instruments) to construct the N_2 adsorption-desorption isotherms. The Brunauer, Emmett, and Teller (BET) methodology was used to evaluate the specific surface area of each GDE sample. The total pore volume was estimated based on the volume adsorbed at the saturation point (P/P_0 = 0.99713) using the Barrett-Joyner-Halenda (BJH) method.

2.5 Set-up for H_2O_2 Electrogeneration and Paracetamol Degradation

The experiments involving the electrogeneration of H_2O_2 and paracetamol (PCT) degradation were conducted in a batch electrochemical reactor with a platinized Ti anode and GDEs prepared as cathodes based on the configuration presented in the supplementary material (Figure SM1). For the electrogeneration of H_2O_2, the electrolyte employed consisted of 0.2L of 0.1 mol L^{-1} K_2SO_4 solution, while the O_2 flow rate (through the GDE) was set at 0.05 L min^{-1}. The potentiostat Metrohm Autolab PGSTAT-302 N was used for the conduct of the experiments, where the following electric currents were tested: 0.15, 0.3, and 0.5 A (*i.e.*, current density (*j)* = 7.5, 15, and 25 mA cm^{-2}, respectively). Initially, the degradation of PCT (20 mg L^{-1}) was evaluated through electrochemical oxidation using the unmodified GDE, 5% Fc-GDE, and 15% Fc-GDE at different current densities (7.5, 15, and 25 mA cm^{-2}). Based on the application of the photo-assisted heterogeneous electro-Fenton treatment process, the unmodified GDE, 5% Fc-GDE, and 15% Fc-GDE were irradiated using 9 W UV-A light (Osram Dulux®S Blue UV-A, 9W/78, maximum emission: 365 nm) at 7.5 mA cm^{-2}. Four control experiments were performed for comparison purposes: i) photolysis (UV-A light, without a cathode), and ii) electrochemical oxidation (EO) using the unmodified GDE, 5% Fc-GDE, and 15% Fc-GDE (under N_2 flow). All the degradation experiments were performed for a period of 90 min. Experiments to capture reactive oxygen species were carried out employing p-benzoquinone (p-BQ, 1 mmol L^{-1}) as scavenger of electron (e^-), superoxide anion radical ($O_2^{\bullet-}$) and $^{\bullet}OH$ [22], ammonium oxalate (AO, 1 mmol L^{-1}) as scavenger of holes (h^+) and isopropyl alcohol (IPA, 100 mmol L^{-1}) as $^{\bullet}OH$ scavenger [23] under identical experimental condition of PCT degradation via photo-assisted heterogeneous electro-Fenton treatment process.

2.6 Analytical procedures

To measure PCT during degradation experiments and radical trapping experiments, firstly, collected aliquots of 1.5 mL were filtered using a Chromafil® Xtra PET filter (0.45

μm). Then, PCT degradation was monitored by high-performance liquid chromatography with a UV-DAD (HPLC-UV/DAD) (Shimadzu Prominence model LC-20AT). The stationary phase was a Phenomenex® Luna C18 column (250 mm × 4.6 mm, 5 μm particle size). The mobile phase consisted of ACN and 0.15 mmol L^{-1} formic acid using a gradient elution mode varying the proportion of AC as follows: from 10% to 60% in 8 min, then from 60 to 100% in 3 min and maintained at 100% for another 3 min (at 1.0 mL min^{-1}). The temperature of column was set at 40°C and 20 μL of injection volume. PCT was detected at 246 nm. The relative percentage of degradation was obtained as $[PCT]/[PCT]_0 \times 100$ %, where [PCT] refers to the values of concentration obtained at a predetermined time and $[PCT]_0$ refers to the initial PCT concentration. Carboxylic acids (acetic, formic, oxalic and oxamic) were identified by HPLC using a Rezek ROA-H™ column from Phenomenex® as the stationary phase and 2.5 mmol L^{-1} H_2SO_4 as the mobile phase at a flow rate of 0.5 mL min^{-1}. The injection volume was 25 μL and temperature was maintained at and 23 °C. The carboxylic acids were detected at 210 nm and identified by comparing their retention times with those of previously analyzed standards.

Total organic carbon concentration ([TOC]) values were analyzed by a Shimadzu model TOC-VCPN and calculated as $(TOC_t/TOC_0) \times 100\%$, with TOC_t representing the values at time *t* and TOC_0 representing the initial TOC value.

The amount of H_2O_2 accumulated was detected spectrophotometrically at 350 nm (Shimadzu UV-1900) by the addition of 0.5 mL of aliquot to 4.0 mL of 2.4 mmol L^{-1} $(NH_4)_2MoO_4$ solution [24, 25]. The iron leached was measured by the 1-10 ortophenantroline colorimetric method at the end of each heterogeneous electro-Fenton and heterogeneous photoelectro-Fenton experiments [26].

2.7 Calculations

The current efficiency (C.E., %) or faradaic efficiency involving the electrogeneration of H_2O_2 was calculated based on Eq. (3) below:

$$C.E.(\%) = \frac{2\,F\,[H_2O_2]V}{I\,t}\,x\,100\% \quad (3)$$

The degradation kinetics of PCT were calculated by fitting the linearized equation of the pseudo-first-order model (Eq. (4)) to the experimental data through linear regression, where C_t represents the concentration values at time t, C_0 represents the initial pollutant concentration, and k_{app} is the apparent rate constant (min^{-1}).

$$-\ln(C_t/C_0)=k_{app} \quad (4)$$

Finally, for a comparison with other EAOPs in terms of cost-efficiency for PCT removal, the figure-of-merit for the electrical energy consumption per order (E_{EO}) was also evaluated using Eq. (5), where 3.84×10^{-2} is a conversion factor (1h/ 60min/0.4343), E is the average potential (in V) of the electrochemical system, P is the nominal power of the UVC lamp and k_{1st} is the pseudo-first order constant (min^{-1}) for the pollutant degradation [27, 28]. Then, it is possible to obtain the amount of kWh of electrical energy required to reduce the contaminant concentration by one order of magnitude (90%) in 1 m^3 of the polluted water.

$$E_{EO}\,(kWh\ m^{-3}order^{-1}) = \frac{3.84\times10^{-2}(E\,I + P)}{k_{1st}\,V} \quad (5)$$

3. Results and Discussion

3.1 Physical and Electrochemical Characterization of GDE and Fc-GDE

The SEM images shown in Figure 1 provide a clear view of the catalytic layer in the unmodified GDE (part a and part e of Figure1) and Fc-modified GDEs (part b,c and part f, g of Figure1). In all the SEM images, one can see that the catalytic layer is effectively impregnated onto the diffusion layer, which is composed of carbon fabric (Figure 1d); the

impregnation gives rise to a compact layer with minimal surface cracks. The small shallow cracks observed in the compact layer are common in these types of electrodes, as the flexible carbon fabric used in the diffusion layer provides some flexibility to the electrode structure; this can occur in the presence of small shallow cracks. It is worth noting that no areas were left uncovered by the catalytic layer across the entire electrode surface. This shows that the layer adheres exceptionally well to the carbon fabric, and this points to one of the advantages of employing the high-pressure technique during GDE preparation at elevated temperatures.

Recently, our research group performed durability tests on these GDE-type electrodes, and the results were highly encouraging [29, 30]. The electrodes exhibited remarkably high lifetime (in terms of current charge passed), where values as high as 48 Ah were obtained when the materials were subjected to high current densities (at 200 mA cm^{-2}). However, over extended periods of use, there was a progressive increase in the thickness of the small shallow cracks. Eventually, this led to the gradual removal of the catalytic layer from the carbon fabric, which became clearly noticeable. It is worth pointing out that the duration of the use of the GDE in our present study was within the expected lifetime of the electrode. Throughout all the experiments conducted, there was no observed decrease in electrode efficiency.

Energy dispersive X-ray spectroscopy (EDS) analyses were performed in order to quantify the amount of Fe metal in the Fc-GDE. The results obtained indicated the presence of Fe metal of approximately 1.8% -3.4%; this is closely in line with the nominal percentage of Fe expected for each electrode. Specifically, for the modified GDE with 5% and 15% Fc content, the theoretical percentages of Fe are 1.5% and 4.5%, respectively. The amounts of Fe recorded in the EDS analyses confirm the successful incorporation of the desired iron content into the Fc-GDE.

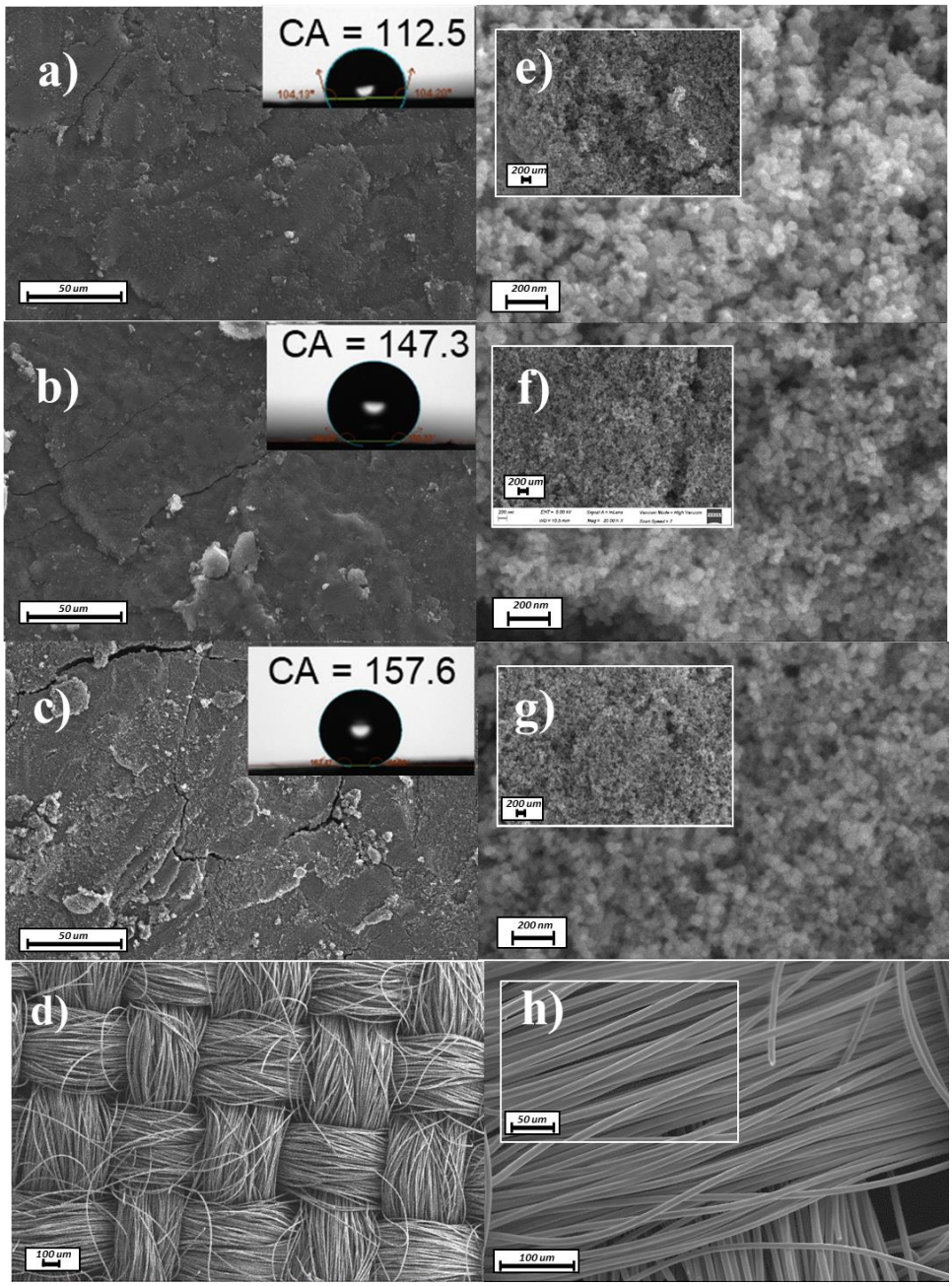

Figure 1. SEM images of the GDEs evaluated: (a) unmodified GDE, (b) 5% Fc-GDE, and (c) 15% Fc-GDE; (h) high magnification of 20,000× of the surfaces of (a), and (b) and (c); (d) bare carbon fabric surface and (h) high magnification of 500× of the bare carbon fabric.

The contact angle analysis was carried out to understand the effect of Fc addition on the surface hydrophobicity of Fc/GDEs compared to unmodified. Inset in Figure 1a-c shows a super hydrophobic feature for 15%Fc GDE (157.6 ± 4.1) and a hydrophobic feature for

5% Fc GDE (147.3 ± 1.2). On the other hand, unmodified GDE presented a contact angle of 112.5 ± 8.5 which indicates a hydrophilic surface. This low interaction with water can be positive to avoid iron leaching from these electrodes.

The X-ray diffractograms obtained for both the unmodified GDE and Fc-GDEs (Figure. 2) exhibited broad diffraction peaks, attributed to amorphous carbon [31], with maximum intensities at 25.6°, 43.4°, and 71.9° are characteristic for the amorphous carbon. A peak at 18° corresponds to the presence of PTFE in the GDE (marked by *). In the case of the Fc-GDEs, no significant variations can be observed. The absence of diffraction peaks related to Fc, suggests the homogeneous incorporation in the PL6C framework. This is in agreement with previous study in literature, in which characteristic peaks of Fc could not be observed after functionalization of graphitic carbon nitride (g-C_3N_4) [23, 32].

Raman analyses of all the GDEs investigated revealed characteristic D and G bands associated with sp^2 and sp^3 hybridized carbons, respectively. The unmodified GDE displayed I_D/I_G ratio of 0.95; this is indicative of an amorphous material with defects in its structure. While this ratio suggests the presence of fewer edge or structural defects compared to highly disordered carbons (where $I_D/I_G > 1$), it does not necessarily imply the absence of defects. Instead, this value aligns with a partially disordered carbon structure, where defects are present but not dominant. It is worth noting that the literature suggests that the presence of defects in carbonaceous materials can help enhance H_2O_2 production during ORR [33, 34].

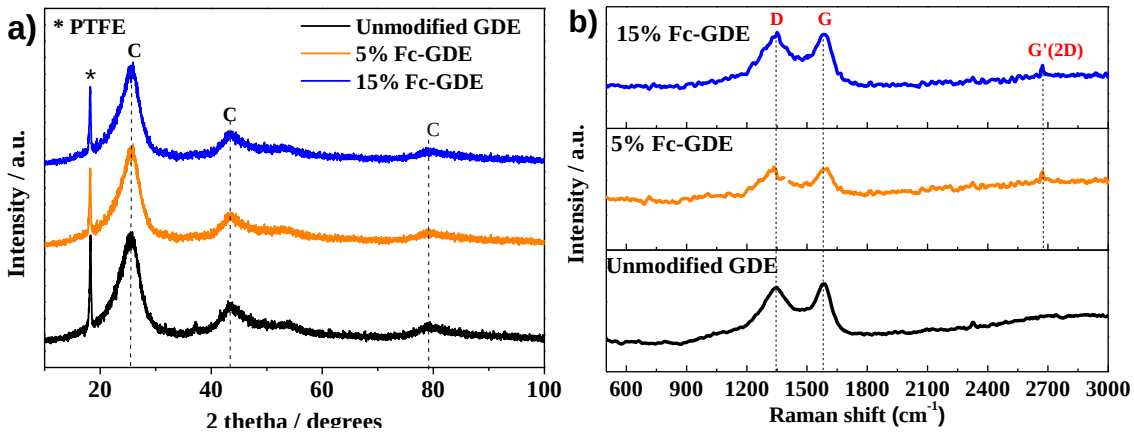

Figure 2. XRD (a) and Raman spectrum (b) of the GDE materials evaluated in this study.

Interestingly, the modified GDEs exhibited I_D/I_G values close to 1.02; this points to levels of crystallinity and defects similar to those of the unmodified electrode. This outcome suggests that the incorporation of Fc does not significantly affect the crystallinity and the structural defects in comparison to the unmodified GDE composition. However, the Raman spectra of the modified GDEs showed a peak corresponding to the 2D band at 2,660 cm^{-1}. This peak arises from the second order scattering of two phonons and may be indicative of long-range order or the number of carbon layers present in the sample [35]; essentially, the aforementioned observation suggests that the cyclopentadienide moiety may exhibit π-π stacking interactions with the sp^2 carbon framework of the PL6C matrix. Potentially, these interactions may subtly reorganize the carbon layers, but not enough to significantly increase the presence of defects. In summary, both modified and unmodified GDE have a comparable balance between crystallinity and defects, and by the incorporation of Fc, it introduces a minor change in the structural proprieties.

To validate the composition and chemical environment, X-ray photoelectron spectroscopy (XPS) analysis was performed on both unmodified GDE samples and those modified with 5.0% ferrocene (5% Fc-GDE). The XPS survey spectra (see Fig SM2 and SM3 of Supporting Information) revealed the presence of major elements including C 1s, O 1s, and F 1s, along with trace amounts of sulfur derived from the Printex L6 amorphous carbon. Notably, no detectable iron signal was observed in the 5% Fc-GDE sample, likely due to its low concentration in the overall chemical composition (Table SM1). As can be observed in the deconvoluted C 1s spectra for the unmodified GDE (Fig 3a) and 5% Fc-GDE (Fig. 3b) the main component at 284.1 eV corresponds to the C=C sp^2 bond of amorphous carbon material (Printex L6 carbon). The relative peak areas were 62.32% for the unmodified GDE and 62.28% for the Fc-GDE, indicating comparable carbon lattice

structures. Both materials also contained similar levels of oxygenated functional groups, predominantly O-C=O bonds, represented by a peak at 286.2 eV. A significant difference between the unmodified and modified GDEs was observed in the π-π* transitions, characterized by a high binding energy peak at 291.5 eV. The Fc GDE exhibited a significantly larger π-π* peak area - approximately twice that of the unmodified GDE (7.6% vs. 3.8%). This finding suggests that ferrocene is effectively anchored to the carbon surface via π-π stacking interactions between its organic cyclopentadienyl rings and the sp^2 carbon matrix.

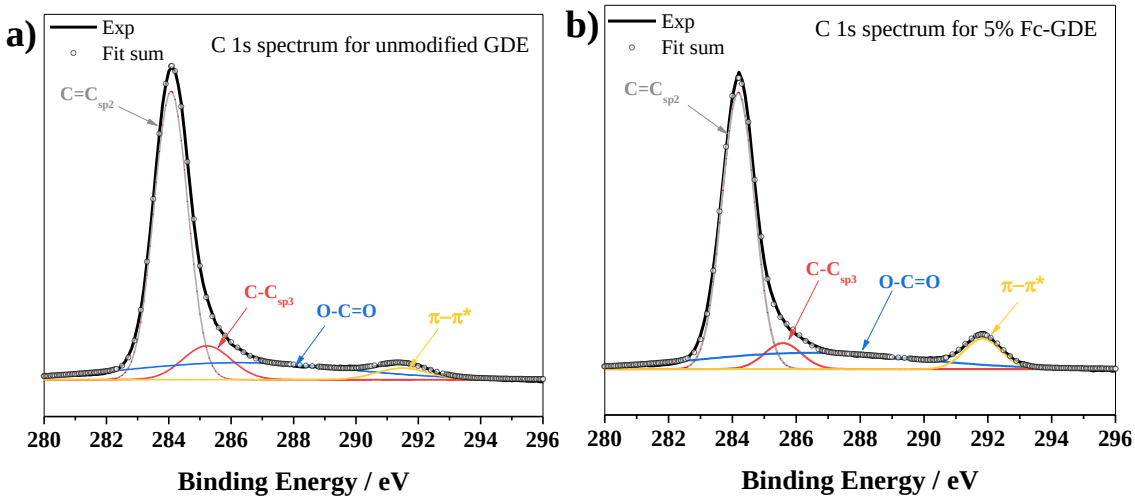

Figure 3. C 1s XPS spectra for (a) unmodified GDE and (b) 5% Fc-GDE.

BET analysis reveals key textural properties of porous materials, including surface area, pore volume and size, which are critical to catalytic efficiency. The results, summarized in Table SM2, allow comparison of these properties. Figure SM4(a) shows the N_2 adsorption-desorption isotherms for the materials. All samples exhibited type IV isotherms, following a consistent trend, with well-defined plateaus indicative of capillary condensation and hysteresis loops (H1). This behavior is associated with porous materials composed of rigid aggregates of uniformly sized spherical particles, a characteristic typical of carbonaceous materials [36-38]. Figure SM4 (b) illustrates the pore size

distribution, complementing the data in Table SM2. The materials demonstrated similar pore sizes, ranging from 12.7 to 19.4 nm, indicative of a predominant microporous and mesoporous structure. This textural characteristic is ideal for the transport of larger molecules, which is desirable for catalytic and adsorption applications. Notably, the 15% Fc material exhibited the highest pore volume (2.09 $cm^3\ g^{-1}$) compared to the PL6C and 5% Fc samples, which explains its elevated specific surface area of 430.8 $m^2\ g^{-1}$ [20, 34, 39, 40].

In addition to surface area analysis via BET analysis, the electrochemically active surface area (ECSA) was estimated for each electrocatalyst from the electrochemical double layer capacitance (C_{dl}) of catalytic microlayer. Cdl values were determined by measuring the non-Faradaic potential capacitive current (i_c) (here at -0.35 V *vs* Ag/AgCl) from CVs recorded at different scan rates, *v* (5 to 150 mV s^{-1}).

Fig SM5a-c shows the CV profiles of PL6C, 5% Fc/PL6C and 15% PLC6 at different scan rates and Fig SM5d shows the plot of ic as function of *v*, and the C_{dl} values, given by $i_c = v\ C_{dl.,}$ where a straight line with a slope equal to C_{dl} is observed. C_{dl} values were of 0.0016mF, 0.0012mF and 0.0009 mF for PL6C, 5% Fc/PL6C and 15% Fc/PL6C, respectively. Then, ECSA values were obtained as the ratio between C_{dl} values and the capacitance of a smooth planar surface per unit area, represented by C_s, corresponding to 0.035 mF cm^{-2} in 1 mol L^{-1} H_2SO_4 ($ECSA=C_{dl}/C_s$) [41]. As observed in Fig SM5e, the ECSA values slightly decreases from 0.45 cm^2 for PL6C to 0.34 cm^2 for 5%Fc/PL6C to 0.25 cm^2 for 15% Fc/PL6C. Is it worth to comment that this method is useful for an internal comparison among materials since the technique is normalized to the employed experimental conditions. This effect in the reduction of ECSA can be related to CA values measured previously (inset in Fig 1a-c). For higher CA values, *i.e.* hydrophobic surfaces, electrolyte molecules penetrates in a lower extent, which in turn may led to the reduced ECSA for modified PL6C matrix, being more pronounced for 15% incorporation. Thus

result is in contrast with BET surface area values for GDEs values, where 15% GDE showed the higher absolute capacity of 7.4-7.8-fold higher compared to 5% Fc GDE and unmodified (PL6C) GDE. As an ex-situ technique using a N_2 gas as probing for surface area, a correlation between BET and ECSA (aqueous electrolyte as probe) is very difficult. In the present study, the highest surface area from BET does not correspond to a higher ECSA, which can be related to the limited electrolyte assess to inner sites of this material [42].

3.2 ORR Characterization using the Hydrodynamic Electrochemical Technique

The cyclic voltammograms shown in Figure SM6 illustrate the behavior of the materials containing only PL6C and the electrodes modified with 5% and 15% of Fc in a stationary system. The voltammograms reveal a distinctive redox wave at 0.2 V vs. Ag/AgCl, which can be attributed to the redox processes associated with the functional oxygenated groups in the carbonaceous matrix. It is worth noting that carbonaceous materials typically exhibit a high capacitive current due to their high electrochemical surface area. In this sense, the redox waves corresponding to Fc were not observed, as they could potentially be overlaid by the high capacitive current of PL6C. Furthermore, when the solution is saturated with O_2, a catalytic wave from the O_2 reduction reaction becomes visible at -0.25 V vs. Ag/AgCl. This peak shows an increase in current intensity and a slight shift toward more positive potentials, when the ferrocene is incorporated into the PL6C. This behavior promotes lower energy consumption for the ORR via the $2e^-$ pathway, indicating that the incorporation of ferrocene into the carbon matrix resulted in a catalytic effect. This effect is attributed to the electronic density shift induced by the interaction between the modifier and the carbon matrix, a phenomenon previously reported in the literature for other compounds, which similarly led to a potential shift in the ORR via the $2e^-$ pathway [16, 43-46].

To better evaluate the performance of the materials in the $2e^-$-ORR, the electrodes were studied using an electrochemical technique in a hydrodynamic system at 900 rpm, where a rotating ring-disk electrode (RRDE) was employed.

Briefly, in this experimental configuration, the disk serves as the cathode where the ORR takes place. The ring acts as a secondary working electrode, oxidizing any H_2O_2 generated at the disk. A fixed positive potential is applied to the ring to selectively oxidize H_2O_2. Thus allowing to analyze the selectivity toward H_2O_2. Meanwhile, the potential of the disk is cathodically swept to study the ORR and the associated electrocatalytic activity. By rotating the RRDE, the hydrodynamic flow directs the ORR products formed at the disk to the ring via convection and diffusion, thus circumventing the issue of H_2O_2 degradation. At the ring, the applied potential of +1.0 V is sufficient to oxidize H_2O_2 without oxidizing H_2O, the secondary product of ORR. This selective oxidation ensures that the detected current at the ring corresponds solely to the oxidation of H_2O_2 and the currents observed at the two electrodes can be used to determine the molar ratio of produced H_2O_2 [19, 47].

Figure 4 presents the disk current values for the PL6C material (represented by the black line) and the materials containing 5% Fc (red line) and 15% Fc (blue line). While the voltammetric profiles for all the materials are similar, the materials containing Fc exhibit a profile shifted towards more positive values. Specifically, the material with 5% Fc displays a shift of 49 mV, whereas the material with 15% Fc exhibits a shift of 64 mV (this behavior can be better observed when one examines Part (a) of Figure SM7). The shift towards more positive values indicates a lower energy requirement for ORR; essentially, this implies that the presence of Fc leads to a considerably greater electrocatalytic effect in ORR and a decrease in energy consumption in the process [48]. By examining the ring currents, which are directly associated with the detection of H_2O_2 generated on the RRDE disk and consequently with the selectivity of ORR, it becomes

evident that the unmodified PL6C material exhibits higher current values for H_2O_2 production, with selectivity of 86.8%. In contrast, the materials modified with Fc display lower selectivity, with selectivity values of 83.3% and 70.4% recorded for Fc contents of 5% and 15% relative to PL6C, respectively (Part (b) of Figure SM7). It is important to highlight that if modified materials showed LSV curves recorded from the disk inclined towards the $4e^-$-ORR pathway, instead of the $2e^-$-ORR, we would observe a substantial increase in the current value on the disk electrode and low current values on the ring electrode. Since this behavior was not observed for materials modified with Fc, this result indicates that Fc plays a dual role: i) it enhances the electrocatalytic effect, as evidenced by the shift in potential towards more positive values, and ii) activates H_2O_2 in radical species, such as $^{\bullet}OH$, as observed in Fenton processes. In this method, H_2O_2 activation is indirectly estimated from the differences in ring's current between PL6C and Fc-containing materials. It has been well established in the literature that Fc can function as a Fenton-like catalyst, capable of activating H_2O_2 to produce $^{\bullet}OH$ species [13, 49, 50]. The incorporation of 15% Fc into the PL6C matrix enhanced the rate of H_2O_2 activation compared to the material containing 5% Fc; this points to a clear relationship between the Fc content and the H_2O_2 activation process. However, when the Fc content exceeds 15%, the incorporation of the catalyst into the carbon matrix becomes uneven, resulting in substantial changes in the material morphology, structure and electrochemical characteristics. Hence, attempts to incorporate higher Fc contents into the carbonaceous matrix proved futile.

It should be noted that the hydrodynamic technique employed in the study provides us with a qualitative analysis. Paracetamol degradation tests were conducted using gas diffusion electrodes in order to have a more conclusive demonstration of the H_2O_2 activation effect facilitated by Fc. The following sections will present a complete discussion of these tests, offering further insights into the results and the relevant findings.

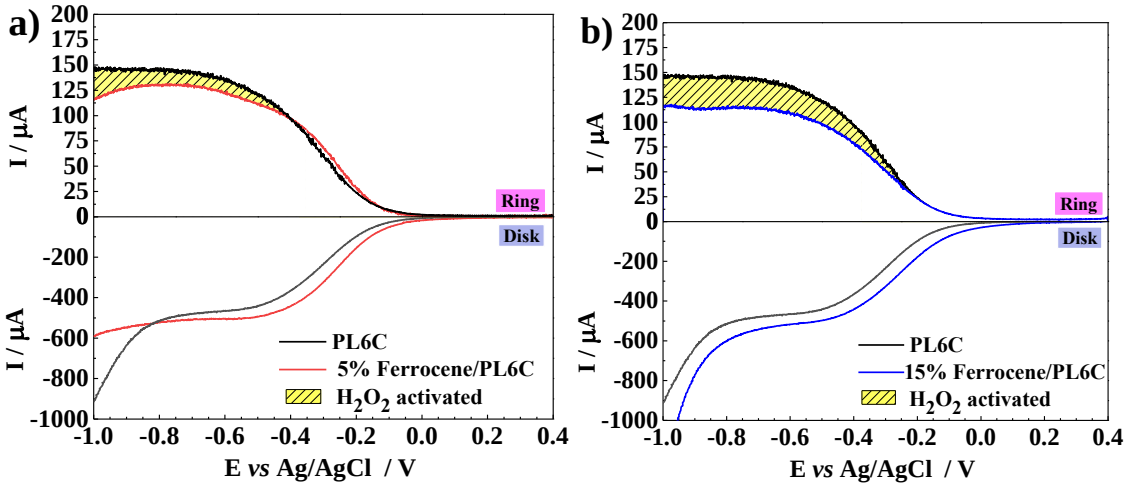

Figure 4. Linear sweep voltammograms obtained for the unmodified PL6C material compared to the (a) 5% Fc/PL6C and (b) 15% Fc/PL6C materials recorded at 900 rpm, based on the application of scan rate of 5 mV s^{-1} and fixed potential of +1.0 V vs. Ag/AgCl applied on the ring (upper panel). Electrolyte: 0.1 mol L^{-1} K_2SO_4 at pH 2.5.

3.3 Electrogeneration of H_2O_2 using GDE

The experiments involving the electrogeneration of H_2O_2 were performed using three different GDEs: unmodified GDE, 5% Fc-GDE, and 15% Fc-GDE. These experiments were carried out in a 0.2 L batch electrochemical cell under galvanostatic conditions and at low current density of 7.5 mA cm^{-2}. The unmodified GDE generated a higher amount of H_2O_2 (105.7 mg L^{-1}) in 90 min of electrolysis, as shown in Fig. 5a, compared to the 5% and 15% Fc-GDEs, which produced 93.3 and 84.2 mg L^{-1} of H_2O_2, respectively. This difference in H_2O_2 production can be attributed to the role of Fc as an activator of H_2O_2, as indicated by the results obtained from the experiments conducted using the hydrodynamic system - RRDE. The Fc-GDEs exhibited a pattern of behavior similar to that observed in the RRDE analysis - incorporating a higher amount of Fc into the carbonaceous matrix helped enhance H_2O_2 activation.

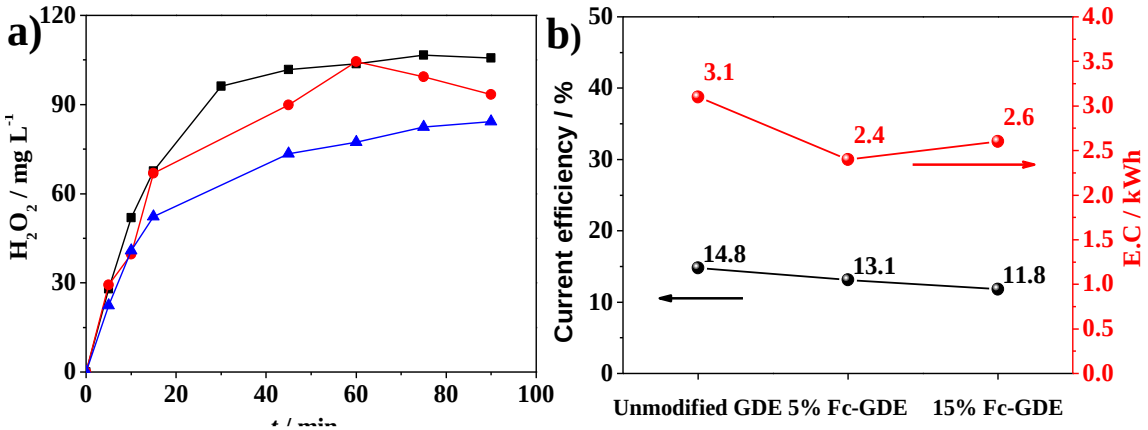

Figure 5. (a) H_2O_2 electrogeneration as a function of reaction time using the unmodified GDE (-■-), 5% Fc-GDE (-●-), and 15% Fc-GDE (-▲-) materials at current density of 7.5 mA cm^{-2}, and (b) current efficiency as a function of the GDE employed. Conditions – electrolyte: 0.1 mol L^{-1} of K_2SO_4; pH =7; temperature = 25 °C.

The results obtained from the experiments conducted showed a linear increase in H_2O_2 concentration during the first 15 min of electrosynthesis. Then, a noticeable stabilization in H_2O_2 electrogeneration was observed after 15 minutes of electrolysis for all GDEs evaluated. This behavior, extensively documented in the literature, is attributed to the establishment of chemical equilibrium between the reactions responsible for H_2O_2 formation at the cathode and those leading to its degradation at the anode [51]. Considering that O_2 and H_2O concentrations are kept constant during the electrogeneration process, one can conclude that the process fits well to a pseudo-zero order kinetics. The kinetic constant (K_{app}) was estimated and the results obtained are summarized in Table SM3. Regarding the current efficiency (C.E.), it can be noted that at 7.5 mA cm^{-2}, the C.E. values obtained vary from 14.8% for the unmodified GDE to 13.1% and 11.8% for the 5% Fc-GDE and 15% Fc-GDEs, respectively (Fig. 5b).

Although the data obtained indicated that the unmodified GDE yielded better results in terms of current efficiency and amount of H_2O_2 electrogenerated, an analysis of the overall energy consumption (EC) (Fig. 5b) showed that the two modified electrodes

recorded relatively lower EC values. This result suggests that greater efficiency of the modified GDEs compared to the unmodified GDE is related to the non-activated H_2O_2 being accumulated whereas the lower energy requirements of Fc GDEs corroborates the finding from RRDE which showed an ORR shift towards more positive values. Taking these results into account, a thorough analysis was conducted in order to evaluate the performance of each GDE when applied for the degradation of PCT; this was done in order to have a better understanding of the effect of modifying the carbon matrix with Fc.

3.4 Degradation of PCT

3.4.1 Effect of Current Density

To evaluate the effect of current density on PCT degradation, three different current densities were tested (7.5, 15, and 25 mA cm^{-2}) using the unmodified GDE, 5% Fc-GDE, and 15% Fc-GDE. Figure 6a-c shows that an increase in current density did not result in a higher rate of PCT degradation for all the GDEs investigated; this was determined by analyzing the charge applied per electrolyzed volume and apparent kinetic rates (k_{app}) (Fig SM8). The result obtained may be attributed to parallel reactions (Eqs. 6-8) that are promoted at elevated current densities [52] and which undermine the smooth occurrence of the main heterogeneous reaction – see Eq. 9 below.

$$2^{\bullet}OH \rightarrow O_2 + 2H^+ + 2e^- \quad (6)$$

$$2^{\bullet}OH \rightarrow H_2O_2 \quad (7)$$

$$H_2O_2 + {}^{\bullet}OH \rightarrow HO_2{}^{\bullet} + H_2O \quad (8)$$

$$Fc^+ + H_2O_2 \rightarrow Fc + {}^{\bullet}OH + OH^- \quad (9)$$

Moreover, as PCT concentration decreases, the processes experiences mass transfer limitations of the contaminant, which competes with the higher amount of intermediates formed during the course of electrolysis, particularly at higher current densities. This phenomenon can also be responsible for the similar degradation rates as current density

increases. A similar behavior was reported in a recent study by Felisardo et al (2024), which investigated the degradation of PCT from urine via electrolysis employing a DSA anode and a stainless-steel foil cathode [53]. They observed that increasing the current density from 6 mA cm^{-2} to 48 mA cm^{-2} resulted in a drop of the oxidation efficiency in the PCT degradation at initial concentration ranging from 5-40 mg L^{-1}, which was attributed to the acceleration of parasitic reactions at the anode, mainly O_2 evolution and preferential attack of the oxidants for the organics presents in the urine matrix.

TOC measurements were performed for samples collected at the end of experiments (90 minutes of electrolysis) for all conditions tested, in order to improve our understanding of the effects of the process involving PCT degradation. The results obtained revealed that the unmodified GDE was only able to remove ~2.0% of TOC, whereas the 5% Fc-GDE and 15% Fc-GDE were able to remove between 3.1 and 3.4% of TOC. This outcome shows that the dual role of the Fc-GDE materials in both H_2O_2 electrogeneration and $^{\bullet}OH$ activation cannot be easily observed due to the minor improvements obtained when they are applied under the conditions investigated. This can be due to the amount of by-products generated (aromatics and carboxylic acids) which requires more time of electrolysis for complete conversion to CO_2.

Finally, the energy requirements for the pollutant removal were estimated for all the systems (Figure 6d) at the current density of 7.5 mA cm^{-2} – the most efficient current density (*j*) when it comes to energy consumption. Under these conditions, the 5% Fc-GDE recorded the most efficient result; this material required only 3.29 kWh m^{-3} $order^{-1}$ to remove an equivalent amount of PCT compared to the other GDEs.

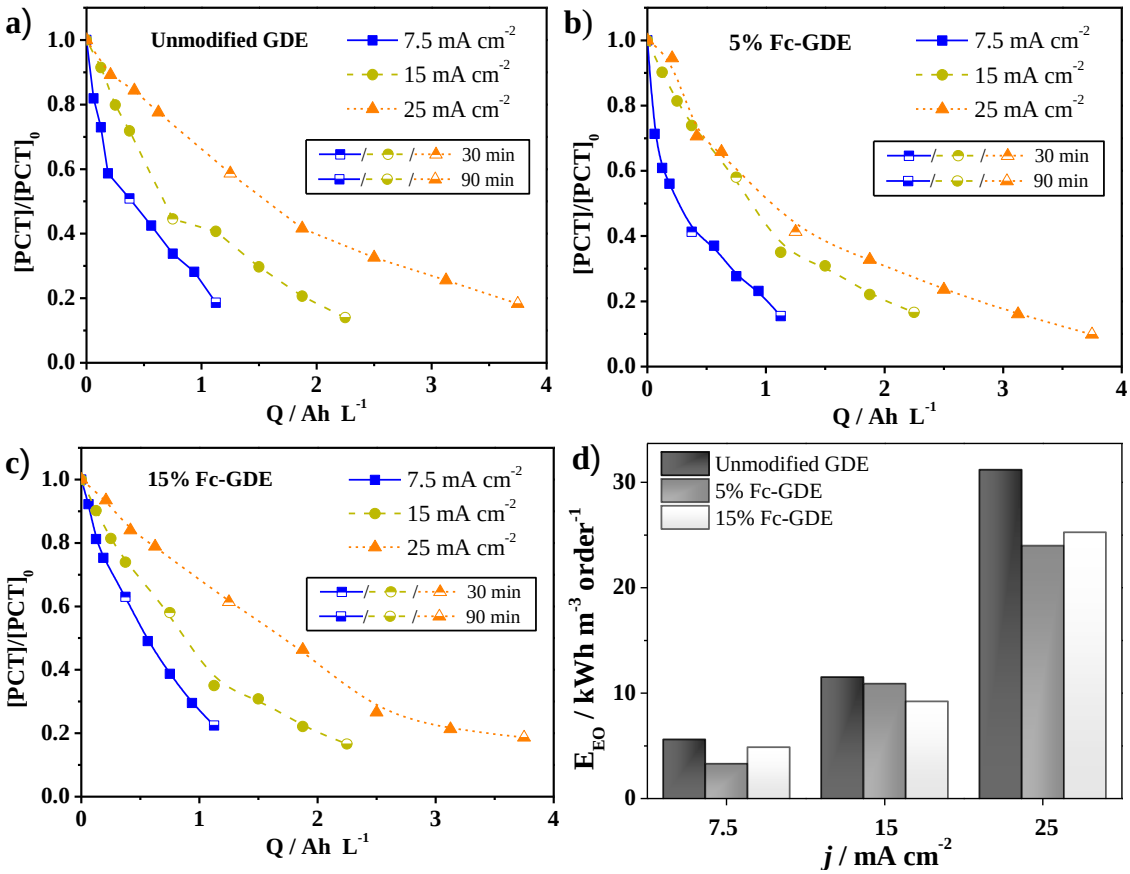

Figure 6. PCT removal as a function of applied electric charge per unit volume for the different cathodic materials tested: (a) unmodified GDE, (b) 5% Fc-GDE, (c) 15% Fc-GDE; and (d) energy consumption per order of contaminant removed. Conditions applied: $[PCT_0]$ = 10 mg L^{-1} ; j = 7.5 mA cm^{-2} ; *time* = 90 min ; pH = 7 ; 0.1 mol L^{-1} K_2SO_4.

3.4.2 Effect of Photolytic Action of UV-A Radiation

Considering that UV-A light can enhance the degradation process, a UV-A lamp was used to irradiate the systems (unmodified GDE, 5% Fc-GDE and 15% Fc-GDE) in order to evaluate their performance in PCT degradation based on the application of the heterogeneous photo-electro-Fenton (EO/H_2O_2/UV-A) process. Initially, a control experiment was carried out; this experiment involved the photolysis of PCT solution (without cathode), followed by the irradiation of the solution. The results obtained from these experiments are shown in Fig. 7a; as can be noted, the PCT molecule was resistant

to UV-A light photolysis, and no noticeable degradation was observed. Experiments under N_2 flow rate are often conducted in order to avoid H_2O_2 generation through O_2 reduction via 2e-ORR and to evaluate the effect of anodic oxidation. However, one needs to point out that PCT can undergo electrochemical reduction on the surface of carbon-based materials - as previously reported in the literature, when it comes to $2e^-/2H^+$ redox reaction [54, 55]. In this context, one is unable to separate the effect of anodic oxidation through the use of an inert gas, such as N_2, since this reaction is favored in the absence of O_2. The batch experimental setup employed in the present study does not allows the use of a membrane to separate anodic and cathodic solutions to evaluate the anodic oxidation effect precisely. However, another configuration was investigated, which consisted of using a stainless steel as cathode plate instead of GDEs. Fig SM9 shows the results obtained from the degradation of PCT during 90 min. As can be observed, PCT efficiency is lower (77.2%) when using stainless steel cathode compared to GDEs (96-99%). This can be due to the higher reduction of PCT on carbon surface. Interestingly, we noticed that the decrease in PCT follows a different trend based on the GDE used; this is clearly indicative of the fact that the modified GDEs are affecting the system, since the anode is kept constant (the same) in all the experiments. Thus, one will observe that PCT is more susceptible to reduction on the surface of the unmodified GDE as opposed to a slower decrease in PCT concentration observed on the surface of the modified GDEs. This outcome may be due to the relatively higher hydrophobicity of the GDEs modified with Fc. Curiously, no changes in TOC were observed irrespective of the GDE employed or stainless steel as cathode; this result confirms that PCT only undergoes conversion in the process.

On the other hand, under O_2 flow in the presence of UV-A irradiation and with the electrogeneration of H_2O_2, the rate of PCT degradation is found to be significantly enhanced (Fig. 7a-b). It is important to note that H_2O_2 exhibits a light absorption band in

the range of 185-300 nm, thus the production of additional •OH is negligible using UV-A (365 nm). Thus, the enhancement of degradation efficiency can be explained by the additional production of •OH by the combination of electro-Fenton-like reaction and UV-A irradiation (heterogeneous photoelectron-Fenton) according to Eq. 10, thus accelerating the degradation of organic pollutants (Eq. 11).

$$Fc + H_2O_2 + h\nu \rightarrow Fc^+ + {}^{\bullet}OH + OH^- \quad (10)$$

$$PCT + {}^{\bullet}OH \rightarrow \text{byproducts} \rightarrow CO_2 + H_2O + \text{inorganic ions} \quad (11)$$

Furthermore, the application of the modified Fc-GDEs led to an increase in TOC removal of approximately 15% (see inset in Fig. 7a).

Although aromatic by-products were not identified, it is possible to follow the decrease in intermediates detected by HPLC at 254 nm as an indicator for the presence of aromatic carbon. This calculation was made considering the ratio between the sum of the peak areas identified after 90 min of electrolysis and the initial peak area of PCT and was carried out for electrolysis carried out at 7.5 mA cm^{-2}. As result, it was observed that 5% GDE and 15% GDE were capable of reduce 67.7% and 62.7% reduction of intermediates peak area compared to 61.1% for unmodified GDE (Fig SM10). This means that with Fc GDEs, faster benzene ring opening to form aliphatic by-products and then short-chain carboxylic acids. The evolution of four short-chain carboxylic acids detected during PCT degradation by EO/H_2O_2/UV-A process was monitored (Fig SM11) After 30 min of electrolysis, oxalic, oxamic and acetid acids were detected for all GDEs employed. Formic acid was detected only during degradation using Fc-GDEs, achieving a maximum in 30 min and then no formic acid was detected at end of experiment. Despite acetic acid was accumulated for all GDEs, its complete removal was achieved only for Fc-GDEs, while remained in the solution for unmodified GDEs. On the other hand, oxamic acid was favored using Fc-GDEs and accumulation followed the same trend regardless GDE;

whereas oxalic acid was accumulated in larger amounts for unmodified GDE. More time should be required to completely degrade these acids and then achieve higher mineralization rates. However, one must consider the lower toxicity of these by-products compared to aromatics.

In terms of energy consumption, once again, the 5% Fc-GDE system proved to be the most energy efficient, as can be seen in Fig. 6c. In view of that, the 5% Fc-GDE was employed under the EO/H_2O_2/UV-A process in order to further investigate another crucial parameter of the system.

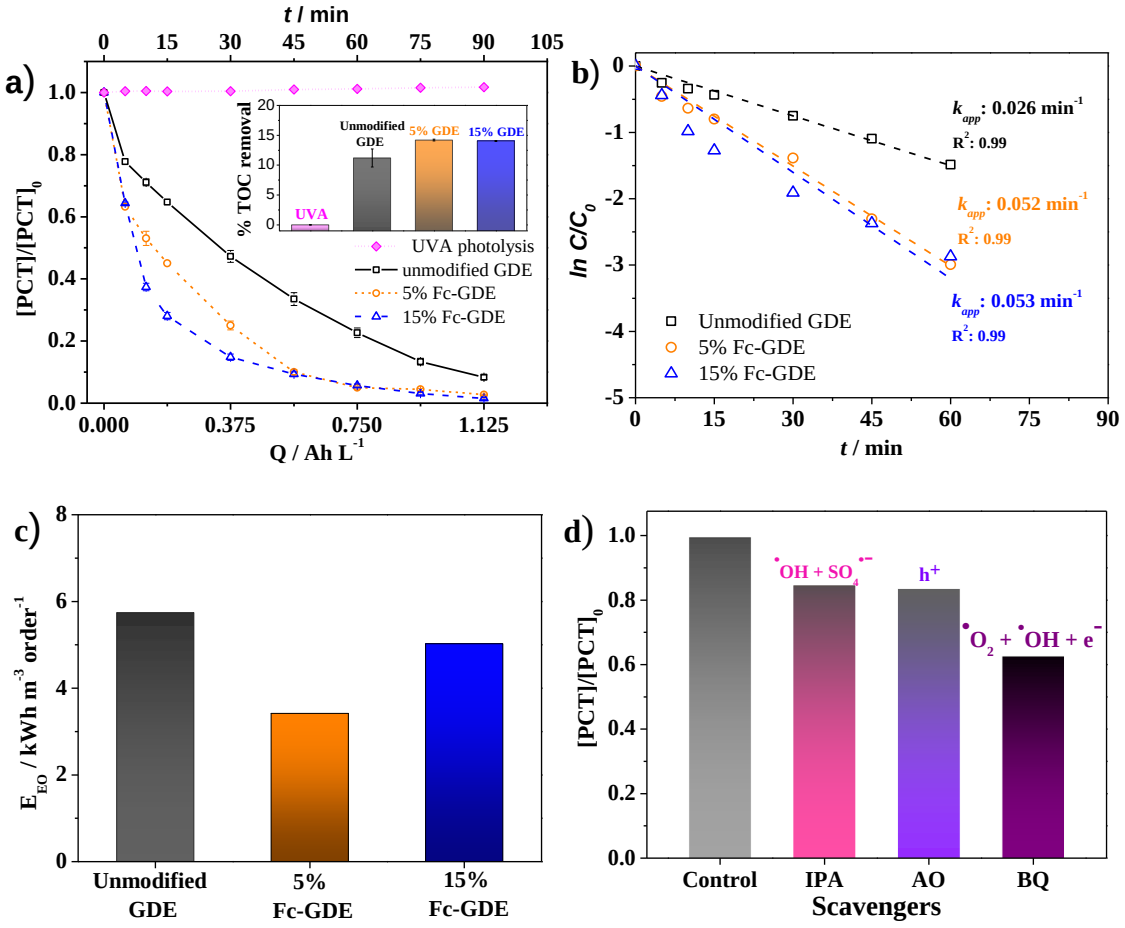

Figure 7. (a) PCT degradation curves obtained from the application of the unmodified GDE and Fc-GDEs under UV-A irradiation under the OE/H_2O_2/UV-A process; (b) kinetic curves, (c) energy consumption per order of the amount of contaminant removed in kWh m^{-3} $order^{-1}$; and (d) quenching experiments conducted during PCT degradation under the OE/H_2O_2/UV-A process using 5% Fc-GDE. Reaction conditions: [PCT_0] = 10 mg L^{-1}; j = 7.5 mA cm^{-2}; pH = 7; duration = 90 min; electrolyte = 0.1 mol L^{-1} K_2SO_4; UV-A = 9 W.

In order to have a comprehensive understanding of the impact of the radical oxygen species (ROS) generated during PCT degradation under the EO/H_2O_2/UV-A process (using the 5% Fc-GDE), different radical scavengers were added into the system, as can be seen in Fig. 7d. In this study, isopropyl alcohol (IPA) was used as scavenger to capture $^{\bullet}OH$ and $SO_4^{\bullet-}$ which presents similar second order constants (2.8×10^9 L mol^{-1} s^{-1} for $^{\bullet}OH$ and 6.0×10^7 L mol^{-1} s^{-1} $SO_4^{\bullet-}$) [23], while ammonium oxalate (OA) was employed as scavenger of h^+. The p-BQ was employed as scavenger of e^- ($0.9–1 \times 10^9$ L mol^{-1} s^{-1}), $O_2^{\bullet-}$ ($0.9–1 \times 10^9$ L mol^{-1} s^{-1}) and $^{\bullet}OH$ (6.6×10^9 L mol^{-1} s^{-1}) [22]. The incorporation of BQ into the system resulted in a reduction of 33% in PCT degradation, while the addition of AO and IPA into the system led to a decrease in PCT degradation of approximately 12% and 11%, respectively. Based on the results obtained from the quenching experiments, it can be concluded that the use of 5% Fc-GDE leads to PCT degradation through various mechanisms: not only on the surface of the cathode and anode but also through UV-A irradiation.

The results obtained in the present study are found to be better than those reported in previous studies on PCT degradation under neutral pH conditions. Using an electrochemical reactor equipped with mesh stainless steel electrodes, Zavala and Estrada (2016) showed that PCT (10 mg L^{-1}) degradation was not favored at pH 7 compared to acid medium, and complete degradation of PCT was only achieved after 240 min (4 h) of

electrolysis at 9.5 mA cm^{-2} [56]. Similarly, Ghanbari et al. (2021) reported to have obtained the highest PCT degradation under the application of ultrasound-assisted heterogeneous electro-Fenton process using 0.15 gL^{-1} Fe_2O_3 nanoparticles at pH 5 and a current density of 230 mA (98.9%) in 60 min of electrolysis; according to the authors, the application of pH 7 and pH 9 led to a significant decrease in degradation percentages. The study conducted by Ghanbari et al. (2021) shows that as the concentration of PCT increases, the rate of PCT degradation decreases in the process due to the fact that higher amounts of oxidizing species are required in order to obtain effective degradation [57]. It is worth noting that suitable electrochemical systems are needed if one seeks to effectively degrade persistent contaminants (such as PCT and other similar pharmaceutical compounds) at a pH close to the level found in most aqueous matrices, since the need for pH adjustment represents one of the major shortcomings of the process.

3.5 Comparison between heterogeneous photo-electro-Fenton and the literature for PCT degradation

Different AOPs technologies has been investigated for PCT degradation, mainly because their efficiency for degradation a wide range of persistent pollutants. In this view, to achieve a better comparison of obtained results in the present work and those from literature, here we summarize the data from selected studies dealing with PCT degradation using Fenton-based approaches [58-62] and other available AOPs such as ozonation [63], electro-peroxone [64] and UV/electrogenerated H_2O_2 [65]. The PCT concentration studied, system employed, conditions applied and removal efficiency are shown in Table 1. Sousa *et al.* 2019 studied the degradation of 100 mg L^{-1} PCT by Fenton-like oxidation employing a carbon/FexOy magnetic composite material from PET and red mud wastes attaining removals values of 40% after 30 min [58]. In another study employing heterogeneous Fenton-like oxidation approach for PCT degradation it was

required 10h to remove 99% of PCT using Cu–Zn–Fe-LDH catalyst at neutral pH [59]. Other study of Van et al 2020 described the heterogenous Fenton oxidation of PCT using iron slag (Fe-S) as catalyst; the removal of PCT at pH 7 after 60 min was 45% for H_2O_2/Fe^{2+} conventional homogeneous reaction and 47% for H_2O_2/Fe-S. In the study of Carrasco-Díaz *et al.* 2017, 85-90% degradation of PCT was achieved in 90 min at pH 3 and 6.2 using Fe-carbon xerogels as heterogeneous catalysts [60]. PCT degradation was also investigated by other AOPs. For example, Trousil et al 2021, described a study comparing ozonation, photolysis and heterogeneous photocatalysis using oxygen or hydrogen peroxide as oxidizing agents for PCT and ibuprofen removal. As result, ibuprofen was better removed than PCT. Moreover, it was demonstrated that direct ozonation was not efficient for PCT degradation, and addition of H_2O_2 (electro-peroxone) does not lead to significant improvement. On the other hand, heterogeneous photocatalysis perfomed better leading to a 64% removal of PCT [63]. On the other hand, Öztürk et al., 2021 investigated the efficiency of different AOPs (ozonation, electro-peroxone, electro-oxidation and goethite catalyzed electro-Fenton) toward PCT degradation and found better outcomes for electro-peroxone and ozonation under conditions studied [64]. Overall, working at mild conditions, that is, 25 °C and pH nearly neutral results in lower kinetic rates during heterogeneous electro-Fenton systems. In particular, the use of ferrocene for degradation of PCT was not yet studied. However, the efficiency of this catalyst in Fenton-like systems has been demonstrated for degradation of several contaminants [REFs]. In the present study we bring the innovation of use of Fc as a modifier in a carbon matrix envisaging degradation of PCT via hetereogeneous photoelectron-Fenton, which can be future expanded for degradation of several organic contaminants. Despite advancements achieved, there is still room for improvements in the process of synthesis of GDEs such as temperature, heating treatment time, pressure applied, solvent for PL6C and Fc dispersion, which was not focus on the present study,

but the feasibility of use GDEs modified with this important and promising heterogeneous catalyst. Advantages of use this strategy includes the use of a reusable electrode and reactions of H_2O_2 generation and activation promoted by the application of low current densities, which makes this process sustainable compared to other classical AOPs.

Table 1. Selected results obtained for different Fenton-based oxidation and other AOPs employed for PCT degradation.

PCT	Process	Conditions	Removal efficiency / %	Ref
Fenton-based oxidation				
100 mg L^{-1}	Adsorption-Fenton-like oxidation	Stirred tank reactor V: 9.8 mL Water matrix: pure water, 10 mg L^{-1} of activated PET-RM catalysts 2 mL of H_2O_2 (30% v/v), T: 25 °C, t: 30 min	40% degradation with PET-RM 800 °C/300min (30 min)	[58]
0.1 mmol L^{-1} (15.1 mg L^{-1})	Heterogeneous Fenton-like oxidation/ adsorption	Stirred tank reactor V: 100 mL Water matrix: pure water [H_2O_2]: 20 mM [Cu–Zn–Fe-LDH]: 0.5 g L^{-1}; pH: 6.0, T: 25 °C, t: 10 h	99% degradation after 10h	[59]
100 mg L^{-1}	Heterogeneous Fenton oxidation	Stirred tank reactor V: 500 mL Water matrix: pure water [H_2O_2]: 100 mg L^{-1} and [Fe^{2+}] or [Fe–S] catalyst: 100 mg L^{-1}; pH 3–11 T: 25 °C, t: 60 min	Degradation by H_2O_2/Fe^{2+}: 51% (pH 3), 45% (pH 7), 28% (pH 11) Degradation by H_2O_2/Fe–S: 53% (pH 3), 47% (pH 7), 25% (pH 11).	[62]
50 mg L^{-1}	Adsorption and Fenton-like oxidation	Stirred tank reactor V: 125 mL Water matrix: pure water [H_2O_2]: 13.8 mg L^{-1}, [Fe-carbon xerogels]: 100 mg L^{-1}, pH 3.0 and 6.2, T: 25 °C, t: 300 min	85-90% degradation in 90 min 45-50% TOC after 300 min	[60]
10 μM (1.5 mg L^{-1})	Heterogeneous Fenton oxidation	Stirred tank reactor V: 250 mL Water matrix: pure water [H_2O_2]: 0.5 mM; [Co–FeOCl]: 0.2 g L^{-1} pH 4, 5.5, 7 and 8.5, T: 25 °C, t: 60 min.	99.3% degradation at pH 4 (k: 0.049 min^{-1}) 76% degradation at pH 8.5 (k: 0.021 min^{-1}) ~80% at pH 5.5 (0.037 min^{-1}) and 7 (0.031 min^{-1})	[61]
20 mg L^{-1}	Heterogeneous photoelectro-Fenton	Stirred tank reactor V: 200 mL; Anode: Ti platinized; Cathode: 5% Fc GDE; O_2 flow: 50 mL min^{-1} Electrolyte: 0.10 M K_2SO_4	95 % degradation in 60 min k: 0.052 min^{-1}	This work

		UV power: 9 W; pH: 7, 25 °C, 90 min Current density: 7.5 mA cm^{-2}		
Other AOPs				
20 mg L^{-1}	Ozonation	Batch recirculation reactor Wastewater flow circulation: 45 L min^{-1} O_3 flow rate: 1 g of O_3 h^{-1} V: 500 mL; pH: 7.2 T: 20° C, t: 60 min	18% degradation 10% TOC reduction	[63]
100 mg L^{-1}	Electro-peroxone	Stirred tank reactor V: 2 L; O_3 flow rate: 5 L min^{-1}; Anode: Pt; Cathode: carbon-PTFE; Electrolyte: 0.50 M Na_2SO_4; pH: 6.8, 25 °C, 60 min Current density: 300 mA	100% degradation in 45 min	[64]
50 mg L^{-1}	UV/electrogenerated H_2O_2	Stirred tank reactor pH: free; UV power: 8 W Anode: Pt coil; Cathode: GDE commercial (5 cm^2) O_2 flow: 100 mL min^{-1} Electrolyte: 0.50 M Na_2SO_4 Current: 50 mA	~100% PCT 16% TOC	[65]

3.5 Leaching

To evaluate and confirm the reusability of the catalyst, we conducted a leaching test in order to measure the concentration of ferrous ions in the solution (Figure 8). The results obtained showed that the concentration of Fe leaching reached its maximum, of 1.8 mg L^{-1}, at a current density of 25 mA cm^{-2} for 5% Fc-GDE. Meanwhile, at lower current densities of 15 and 7.5 mA cm^{-2}, the concentrations of Fe leaching recorded were only 0.06 and 0.2 mg L^{-1}, respectively, for 5% Fc GDE. Furthermore, the concentration of Fe leaching recorded under UV-A irradiation was 0.6 mg L^{-1} for 5% Fc-GDE and 0.9 mg L^{-1} for 15% Fc-GDE; this outcome can be associated with the photo-reduction of Fe^{3+} to Fe^{2+}, where the latter is soluble in water, so the species can be detected in higher concentrations. The Fe leaching concentration values recorded in this study are lower than the recommended maximum concentration (RMC) of Fe recommended by the World Health Organization (WHO) for water reutilization in crop irrigation, which is 5 mg L^{-1}. In general, standard of iron for irrigation purposes does not differ significantly among the countries [66]. For example, Taiwan, Egypt, Saudi Arabia, Tunisia also consider 5 mg L^{-}

[1] as the limit, whereas Israel and Italy considers 2 mg L^{-1}. The US has different standards for irrigation according to the time of exposure, being 5 mg L^{-1} for long term and 20 mg L^{-1} for short term. However, the irradiated processes do not meet the maximum permissible limit for drinking water which is 0.3 mg L^{-1} as established by the World Health Organization (WHO), Food and Agriculture Organization (FAO) and United States Environmental Protection Agency (USEPA). Standards for human consumption recommended by European Union standard is 0.0002 mg L^{-1}.

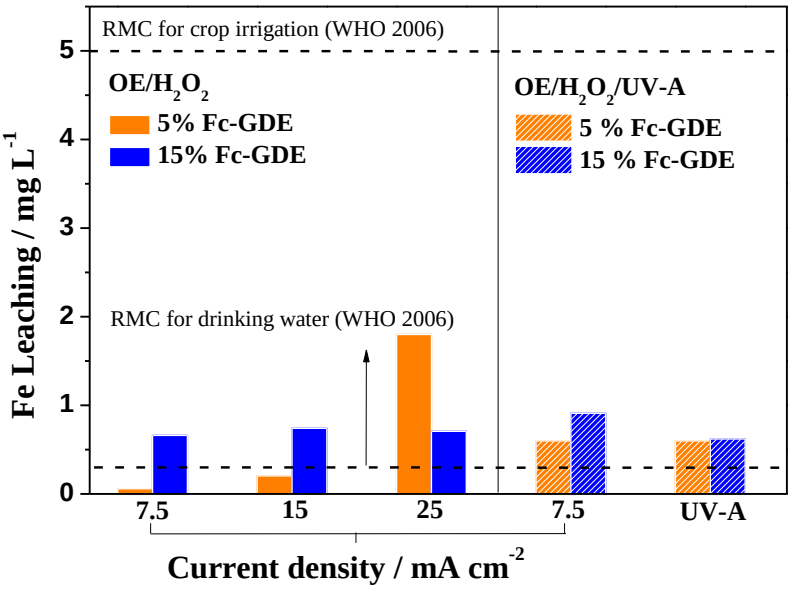

Figure 8. Iron leaching after PCT degradation based on the application of Fc-GDEs under different conditions. Reaction conditions: [PCT_0] = 10 mg L^{-1}; pH = 7; *time* = 90 min; electrolyte = 0.1 mol L^{-1} K_2SO_4; UV-A = 9 W.

Finally, the results obtained in the study showed that the 5% Fc-GDE is the optimal material among the GDEs tested in terms of lower current densities and energy consumption. The findings of the study show that the modification of carbon-based GDEs with ferrocene leads to the development of a highly efficient material with good properties that are suitable for PCT degradation. The ferrocene-modified GDE proposed in this study is highly promising, has good application potential and needs to be explored further in flow reactors [67, 68].

4. Conclusions

In the present work, the main conclusions can be drawn:

- We reported, for the first time, the development of a novel gas diffusion electrode modified with different amounts of Fc and successful incorporation was confirmed by using physical characterization (SEM-EDS, Raman and contact angle).
- The electrochemical characterization conducted using the RRDE technique pointed to a decrease in the amount of H_2O_2 detected in the ring; this outcome may be related to the conversion of H_2O_2 to $^{\bullet}OH$, a process catalyzed by the presence of Fe.
- It was demonstrated the successful application of Fc-GDEs for the effective treatment of water contaminated with paracetamol. Unmodified and modified GDEs for paracetamol degradation showed that 7.5 mA cm^{-2} is the most efficient current density, as it yielded the best outcome among the current densities evaluated.
- The application of UV-A irradiation led to significant improvements in the degradation efficiency, especially for the 15% Fc-GDE; this can be explained by the interaction of Fc with UV-A light, which led to the formation of additional $^{\bullet}OH$ species. However, 5% Fc-GDE appears to be the most suitable cathode among the GDEs investigated, as it yielded best outcomes in terms of energy consumption and TOC removal.
- The low iron leaching detected after the use of the 5% Fc-GDE represents a great advance in heterogeneous electro-Fenton, showing that this electrode can be used for the efficient degradation of pharmaceutical compounds in neutral water

matrices, and this can help ensure the safety and quality of water to be reused for crop irrigation, among other purposes.

Finally, the application of ferrocene-modified carbon-based GDEs for the treatment of real water matrices has great application potential and needs to be further investigated in flow reactors.

Acknowledgments

This study was financed, in part, by the São Paulo Research Foundation (FAPESP), Brasil. Process Number #2018/22211-7, #2018/22210-0, #2018/22022-0, #2019/06650-3, #2020/02743-4, #2022/03386-6, #2020/07351-7 #2022/07227-0, #2016/19612-4, and #2022/12895-1. The authors also acknowledge the funding received by the Brazilian National Council for Scientific and Technological Development (CNPq – grant #303943/2021-1) and the financial support received from PDC2021-121105-I00 granted by MCIN/ AEI/10.13039/501100011033/ and "Unión Europea Next Generation EU/PRTR".

Declaration of competing interest

The authors declare that they have no known competing financial interests or personal relationships that may have influenced the work reported in this paper.

Credit author statement

Géssica O. S. Santos: writing – original draft, investigation, validation, formal analysis. **Isaac Sánchez-Montes:** writing – original draft, investigation, validation, formal analysis. **Paulo Jorge M. Cordeiro-Junior:** writing – original draft, investigation, validation, formal analysis. **Taynara O. Silva:** investigation, validation, formal analysis.

M. A. Rodrigo: conceptualization, supervision, writing – review and editing. **Marcos R.**

V. Lanza: formal analysis, supervision, funding acquisition, writing – review and editing.

References

[1] E.O. Reis, A.F.S. Foureaux, J.S. Rodrigues, V.R. Moreira, Y.A. Lebron, L.V. Santos, M.C. Amaral, L.C. Lange, Occurrence, removal and seasonal variation of pharmaceuticals in Brasilian drinking water treatment plants, Environmental Pollution, 250 (2019) 773-781.
[2] M. Ashfaq, Y. Li, M.S.U. Rehman, M. Zubair, G. Mustafa, M.F. Nazar, C.-P. Yu, Q. Sun, Occurrence, spatial variation and risk assessment of pharmaceuticals and personal care products in urban wastewater, canal surface water, and their sediments: A case study of Lahore, Pakistan, Science of The Total Environment, 688 (2019) 653-663.
[3] Y. Yang, Y.S. Ok, K.-H. Kim, E.E. Kwon, Y.F. Tsang, Occurrences and removal of pharmaceuticals and personal care products (PPCPs) in drinking water and water/sewage treatment plants: A review, Science of the Total Environment, 596 (2017) 303-320.
[4] S. Wu, L. Zhang, J. Chen, Paracetamol in the environment and its degradation by microorganisms, Applied microbiology and biotechnology, 96 (2012) 875-884.
[5] G.O. Santos, L.A. Goulart, P.J. Cordeiro-Junior, I. Sánchez-Montes, M.R. Lanza, Pharmaceutical contaminants: ecotoxicological aspects and recent advances in oxidation technologies for their removal in aqueous matrices, Journal of Environmental Chemical Engineering, (2022) 108932.
[6] E. Brillas, I. Sirés, M.A. Oturan, Electro-Fenton process and related electrochemical technologies based on Fenton's reaction chemistry, Chemical reviews, 109 (2009) 6570-6631.
[7] T. Shi, J. Peng, J. Chen, C. Sun, H. He, Heterogeneous photo-fenton degradation of norfloxacin with Fe3O4-multiwalled carbon nanotubes in aqueous solution, Catalysis Letters, 147 (2017) 1598-1607.
[8] V. Poza-Nogueiras, E. Rosales, M. Pazos, M.A. Sanroman, Current advances and trends in electro-Fenton process using heterogeneous catalysts–a review, Chemosphere, 201 (2018) 399-416.
[9] H. Luo, Y. Zeng, D. He, X. Pan, Application of iron-based materials in heterogeneous advanced oxidation processes for wastewater treatment: A review, Chemical Engineering Journal, 407 (2021) 127191.
[10] S.O. Ganiyu, T.X.H. Le, M. Bechelany, G. Esposito, E.D. van Hullebusch, M.A. Oturan, M. Cretin, A hierarchical CoFe-layered double hydroxide modified carbon-felt cathode for heterogeneous electro-Fenton process, Journal of Materials Chemistry A, 5 (2017) 3655-3666.
[11] Q. Wang, S. Tian, P. Ning, Degradation mechanism of methylene blue in a heterogeneous Fenton-like reaction catalyzed by ferrocene, Industrial & Engineering Chemistry Research, 53 (2014) 643-649.
[12] Q. Wang, S. Tian, J. Cun, P. Ning, Degradation of methylene blue using a heterogeneous Fenton process catalyzed by ferrocene, Desalination and Water Treatment, 51 (2013) 5821-5830.
[13] G. Divyapriya, I. Nambi, J. Senthilnathan, Ferrocene functionalized graphene based electrode for the electro− Fenton oxidation of ciprofloxacin, Chemosphere, 209 (2018) 113-123.
[14] Z. Huang, H. Yu, L. Wang, X. Liu, S. Ren, J. Liu, Ferrocene-modified Uio-66-NH_2 hybrids with g-C_3N_4 as enhanced photocatalysts for degradation of bisphenol A under visible light, Journal of Hazardous Materials, 436 (2022) 129052.
[15] G.O. Santos, P.J. Cordeiro-Junior, I. Sánchez-Montes, R.S. Souto, M.S. Kronka, M.R. Lanza, Recent advances in H_2O_2 electrosynthesis based on the application of gas diffusion electrodes: challenges and opportunities, Current Opinion in Electrochemistry, (2022) 101124.

[16] J. Moreira, V.B. Lima, L.A. Goulart, M.R. Lanza, Electrosynthesis of hydrogen peroxide using modified gas diffusion electrodes (MGDE) for environmental applications: Quinones and azo compounds employed as redox modifiers, Applied Catalysis B: Environmental, 248 (2019) 95-107.
[17] I. Sánchez-Montes, G.O. Santos, T.O. Silva, R. Colombo, M.R. Lanza, An innovative approach to the application of electrochemical processes based on the in-situ generation of H_2O_2 for water treatment, Journal of Cleaner Production, 392 (2023) 136242.
[18] T.O. Silva, G.d.O.S. Santos, R. Colombo, M.R. de Vasconcelos Lanza, M.A.R. Rodrigo, Degradation of diethyl phthalate by photolysis of hydrogen peroxide electrogenerated using a Printex L6 carbon modified with Benzophenone cathode in an improved tangential flow cell, Process Safety and Environmental Protection, (2024).
[19] C. Du, Y. Sun, T. Shen, G. Yin, J. Zhang, Applications of RDE and RRDE methods in oxygen reduction reaction, Rotating Electrode Methods and Oxygen Reduction Electrocatalysts, (2014) 231-277.
[20] P.J.M. Cordeiro-Junior, M.S. Kronka, L.A. Goulart, N.C. Veríssimo, L.H. Mascaro, M.C. dos Santos, R. Bertazzoli, M.R. de Vasconcelos Lanza, Catalysis of oxygen reduction reaction for H_2O_2 electrogeneration: The impact of different conductive carbon matrices and their physicochemical properties, Journal of Catalysis, 392 (2020) 56-68.
[21] P.J.M. Cordeiro-Junior, M.R. de Vasconcelos Lanza, M.A.R. Rodrigo, Modeling the electrosynthesis of H_2O_2: Understanding the role of predatory species, Chemical Engineering Science, (2023) 118647.
[22] E.M. Rodriguez, G. Marquez, M. Tena, P.M. Álvarez, F.J. Beltrán, Determination of main species involved in the first steps of TiO_2 photocatalytic degradation of organics with the use of scavengers: The case of ofloxacin, Applied Catalysis B: Environmental, 178 (2015) 44-53.
[23] I. Sánchez-Montes, J.C. Doerenkamp, Y. Núñez-de la Rosa, P. Hammer, R.C. Rocha-Filho, J.M. Aquino, Effective Fenton-like degradation of the tebuthiuron herbicide by ferrocene functionalized g-C_3N_4, Journal of Photochemistry and Photobiology A: Chemistry, 435 (2023) 114276.
[24] X.-S. Chai, Q. Hou, Q. Luo, J. Zhu, Rapid determination of hydrogen peroxide in the wood pulp bleaching streams by a dual-wavelength spectroscopic method, Analytica chimica acta, 507 (2004) 281-284.
[25] P.J.M. Cordeiro-Junior, A.S. Martins, G.B.S. Pereira, F.V. Rocha, M.A.R. Rodrigo, M.R. de Vasconcelos Lanza, Bisphenol-S removal via photoelectro-fenton/H_2O_2 process using Co-porphyrin/Printex L6 gas diffusion electrode, Separation and Purification Technology, 285 (2022) 120299.
[26] G.K. Murti, A. Moharir, V. Sarma, Spectrophotometric determination of iron with orthophenanthroline, Microchemical Journal, 15 (1970) 585-589.
[27] J.R. Bolton, K.G. Bircher, W. Tumas, C.A. Tolman, Figures-of-Merit for the Technical Development and Application of Advanced Oxidation Processes, Journal of Advanced Oxidation Technologies, 1 (1996) 13-17.
[28] M. Lanzarini-Lopes, S. Garcia-Segura, K. Hristovski, P. Westerhoff, Electrical energy per order and current efficiency for electrochemical oxidation of p-chlorobenzoic acid with boron-doped diamond anode, Chemosphere, 188 (2017) 304-311.
[29] P.J.M. Cordeiro-Junior, J. Lobato Bajo, M.R.d.V. Lanza, M.A.s. Rodrigo Rodrigo, Highly Efficient Electrochemical Production of Hydrogen Peroxide Using the GDE Technology, Industrial & Engineering Chemistry Research, 61 (2022) 10660-10669.
[30] P.J.M. Cordeiro-Junior, C.S. Jiménez, M.R. de Vasconcelos Lanza, M.A.R. Rodrigo, Electrochemical production of extremely high concentrations of hydrogen peroxide in discontinuous processes, Separation and Purification Technology, 300 (2022) 121847.
[31] A. Sadezky, H. Muckenhuber, H. Grothe, R. Niessner, U. Pöschl, Raman microspectroscopy of soot and related carbonaceous materials: Spectral analysis and structural information, Carbon, 43 (2005) 1731-1742.
[32] K.-Y.A. Lin, J.-T. Lin, Ferrocene-functionalized graphitic carbon nitride as an enhanced heterogeneous catalyst of Fenton reaction for degradation of Rhodamine B under visible light irradiation, Chemosphere, 182 (2017) 54-64.

[33] H. Zhang, Y. Li, Y. Zhao, G. Li, F. Zhang, Carbon black oxidized by air calcination for enhanced H_2O_2 generation and effective organics degradation, ACS applied materials & interfaces, 11 (2019) 27846-27853.
[34] Y. Liu, X. Quan, X. Fan, H. Wang, S. Chen, High-yield electrosynthesis of hydrogen peroxide from oxygen reduction by hierarchically porous carbon, Angewandte Chemie, 127 (2015) 6941-6945.
[35] J.H. Lehman, M. Terrones, E. Mansfield, K.E. Hurst, V. Meunier, Evaluating the characteristics of multiwall carbon nanotubes, Carbon, 49 (2011) 2581-2602.
[36] K.S. Sing, Reporting physisorption data for gas/solid systems with special reference to the determination of surface area and porosity (Provisional), Pure and applied chemistry, 54 (1982) 2201-2218.
[37] M. Inagaki, H. Konno, O. Tanaike, Carbon materials for electrochemical capacitors, Journal of power sources, 195 (2010) 7880-7903.
[38] Y. Sun, I. Sinev, W. Ju, A. Bergmann, S. Dresp, S. Kuhl, C. Spori, H. Schmies, H. Wang, D. Bernsmeier, Efficient electrochemical hydrogen peroxide production from molecular oxygen on nitrogen-doped mesoporous carbon catalysts, Acs Catalysis, 8 (2018) 2844-2856.
[39] W. Zhou, L. Rajic, L. Chen, K. Kou, Y. Ding, X. Meng, Y. Wang, B. Mulaw, J. Gao, Y. Qin, Activated carbon as effective cathode material in iron-free Electro-Fenton process: Integrated H_2O_2 electrogeneration, activation, and pollutants adsorption, Electrochimica acta, 296 (2019) 317-326.
[40] J.J. Lado, R.L. Zornitta, F.A. Calvi, M.I. Tejedor-Tejedor, M.A. Anderson, L.A. Ruotolo, Study of sugar cane bagasse fly ash as electrode material for capacitive deionization, Journal of Analytical and Applied Pyrolysis, 120 (2016) 389-398.
[41] C.C. McCrory, S. Jung, J.C. Peters, T.F. Jaramillo, Benchmarking heterogeneous electrocatalysts for the oxygen evolution reaction, Journal of the American Chemical Society, 135 (2013) 16977-16987.
[42] S. Trasatti, O. Petrii, Real surface area measurements in electrochemistry, Pure and applied chemistry, 63 (1991) 711-734.
[43] Y. Bu, Y. Wang, G.F. Han, Y. Zhao, X. Ge, F. Li, Z. Zhang, Q. Zhong, J.B. Baek, Carbon-based electrocatalysts for efficient hydrogen peroxide production, Advanced Materials, 33 (2021) 2103266.
[44] J. Forti, R. Rocha, M. Lanza, R. Bertazzoli, Electrochemical synthesis of hydrogen peroxide on oxygen-fed graphite/PTFE electrodes modified by 2-ethylanthraquinone, Journal of Electroanalytical Chemistry, 601 (2007) 63-67.
[45] E. Yeager, Electrocatalysts for O_2 reduction, Electrochimica Acta, 29 (1984) 1527-1537.
[46] P.J.M.C. Junior, R.S. Souto, M. de Oliveira Almeida, G.B.S. Pereira, M.A. Franco, K.M. Honorio, F.V. Rocha, M.R. de Vasconcelos Lanza, A combined approach toward enhancing 2-electron oxygen reduction through the incorporation of Pd-based complex into a carbonaceous matrix: experimental and mechanistic-theoretical studies, Electrochimica Acta, 460 (2023) 142543.
[47] X. Shi, S. Back, T.M. Gill, S. Siahrostami, X. Zheng, Electrochemical synthesis of H2O2 by two-electron water oxidation reaction, Chem, 7 (2021) 38-63.
[48] J.F. Carneiro, L.C. Trevelin, A.S. Lima, G.N. Meloni, M. Bertotti, P. Hammer, R. Bertazzoli, M.R. Lanza, Synthesis and characterization of ZrO_2/C as electrocatalyst for oxygen reduction to H_2O_2, Electrocatalysis, 8 (2017) 189-195.
[49] Q. Wang, S. Tian, P. Ning, Ferrocene-Catalyzed heterogeneous fenton-like degradation of methylene blue: influence of initial solution pH, Industrial & Engineering Chemistry Research, 53 (2014) 6334-6340.
[50] Y. Li, B. Zhang, X. Liu, Q. Zhao, H. Zhang, Y. Zhang, P. Ning, S. Tian, Ferrocene-catalyzed heterogeneous Fenton-like degradation mechanisms and pathways of antibiotics under simulated sunlight: a case study of sulfamethoxazole, Journal of hazardous materials, 353 (2018) 26-34.
[51] T.O. Silva, L.A. Goulart, I. Sánchez-Montes, G.O. Santos, R.B. Santos, R. Colombo, M.R. Lanza, Using a novel gas diffusion electrode based on PL6 carbon modified with benzophenone for efficient H_2O_2 electrogeneration and degradation of ciprofloxacin, Chemical Engineering Journal, 455 (2023) 140697.
[52] P. Nidheesh, R. Gandhimathi, Trends in electro-Fenton process for water and wastewater treatment: an overview, Desalination, 299 (2012) 1-15.

[53] R.J.A. Felisardo, E. Brillas, T.H. Boyer, E.B. Cavalcanti, S. Garcia-Segura, Electrochemical degradation of acetaminophen in urine matrices: Unraveling complexity and implications for realistic treatment strategies, Water Research, 261 (2024) 122034.
[54] B. Healy, F. Rizzuto, M. de Rose, T. Yu, C.B. Breslin, Electrochemical determination of acetaminophen at a carbon electrode modified in the presence of β-cyclodextrin: role of the activated glassy carbon and the electropolymerised β-cyclodextrin, Journal of Solid State Electrochemistry, 25 (2021) 2599-2609.
[55] X. Chen, J. Zhu, Q. Xi, W. Yang, A high performance electrochemical sensor for acetaminophen based on single-walled carbon nanotube–graphene nanosheet hybrid films, Sensors and Actuators B: Chemical, 161 (2012) 648-654.
[56] M.Á. López Zavala, E. Espinoza Estrada, Degradation of acetaminophen and its transformation products in aqueous solutions by using an electrochemical oxidation cell with stainless steel electrodes, Water, 8 (2016) 383.
[57] F. Ghanbari, A. Hassani, S. Wacławek, Z. Wang, G. Matyszczak, K.-Y.A. Lin, M. Dolatabadi, Insights into paracetamol degradation in aqueous solutions by ultrasound-assisted heterogeneous electro-Fenton process: Key operating parameters, mineralization and toxicity assessment, Separation and Purification Technology, 266 (2021) 118533.
[58] L.S. Sousa, P. Chagas, L.C.A. de Oliveira, C.S. de Castro, Carbon/Fe_xO_y magnetic composites obtained from PET and red mud residues: paracetamol and dye oxidation, Environmental technology, (2019).
[59] H. Lu, Z. Zhu, H. Zhang, J. Zhu, Y. Qiu, L. Zhu, S. Küppers, Fenton-like catalysis and oxidation/adsorption performances of acetaminophen and arsenic pollutants in water on a multimetal Cu–Zn–Fe-LDH, ACS applied materials & interfaces, 8 (2016) 25343-25352.
[60] M.R. Carrasco-Díaz, E. Castillejos-López, A. Cerpa-Naranjo, M.L. Rojas-Cervantes, On the textural and crystalline properties of Fe-carbon xerogels. Application as Fenton-like catalysts in the oxidation of paracetamol by H_2O_2, Microporous and Mesoporous Materials, 237 (2017) 282-293.
[61] C. Tan, T. Sheng, Q. Xu, T. Xu, K. Sun, L. Deng, W. Xu, Cobalt doped iron oxychloride as efficient heterogeneous Fenton catalyst for degradation of paracetamol and phenacetin, Chemosphere, 263 (2021) 127989.
[62] H.T. Van, L.H. Nguyen, T.K. Hoang, T.T. Nguyen, T.N.H. Tran, T.B.H. Nguyen, X.H. Vu, M.T. Pham, T.P. Tran, T. Pham, Heterogeneous Fenton oxidation of paracetamol in aqueous solution using iron slag as a catalyst: Degradation mechanisms and kinetics, Environmental Technology & Innovation, 18 (2020) 100670.
[63] V. Trousil, J. Palarčík, Z. Blažková, J. Kořínková, O. Machalický, J. Cakl, Paracetamol and ibuprofen removal from aqueous solutions by ozonation and photochemical processes, (2018).
[64] H. Öztürk, S. Barışçı, O. Turkay, Paracetamol degradation and kinetics by advanced oxidation processes (AOPs): Electro-peroxone, ozonation, goethite catalyzed electro-fenton and electro-oxidation, Environmental Engineering Research, 26 (2021).
[65] I. Bavasso, C. Poggi, E. Petrucci, Enhanced degradation of paracetamol by combining UV with electrogenerated hydrogen peroxide and ozone, Journal of Water Process Engineering, 34 (2020) 101102.
[66] C.-Y. Chen, S.-W. Wang, H. Kim, S.-Y. Pan, C. Fan, Y.J. Lin, Non-conventional water reuse in agriculture: A circular water economy, Water Research, 199 (2021) 117193.
[67] J.F. Pérez, J. Llanos, C. Sáez, C. López, P. Cañizares, M.A. Rodrigo, Towards the scale up of a pressurized-jet microfluidic flow-through reactor for cost-effective electro-generation of H_2O_2, Journal of Cleaner Production, 211 (2019) 1259-1267.
[68] C. Zhang, G. Ren, W. Wang, X. Yu, F. Yu, Q. Zhang, M. Zhou, A new type of continuous-flow heterogeneous electro-Fenton reactor for Tartrazine degradation, Separation and Purification Technology, 208 (2019) 76-82.